Acta Cryst E CRYSTALLOGRAPHIC COMMUNICATIONS

ISSN 2056-9890

Crystal structure and Hirshfeld surface analysis of (*E*)-3-(3-iodophenyl)-1-(4-iodophenyl)prop-2-en-1-one

Kieran J. Spruce,[a] Charlie L. Hall,[a]* Jason Potticary,[a] Natalie E. Pridmore,[a] Matthew E. Cremeens,[b] Gemma D. D'ambruoso,[b] Masaomi Matsumoto,[b] Gabrielle I. Warren,[b] Stephen D. Warren[b] and Simon R. Hall[a]

[a]School of Chemistry, University of Bristol, Cantock's Close, Bristol, England, BS8 1TS, England, and [b]Department of Chemistry & Biochemistry, Gonzaga University, 502 E Boone Ave, Spokane, WA 99258, USA. *Correspondence e-mail: simon.hall@bristol.ac.uk

Received 13 November 2019
Accepted 5 December 2019

Edited by H. Ishida, Okayama University, Japan

Keywords: crystal structure; *E* configuration; iodophenyl ring; chalcone; (*E*)-3-(3-iodophenyl)-1-(4-iodophenyl)prop-2-en-1-one.

CCDC reference: 1970266

Supporting information: this article has supporting information at journals.iucr.org/e

The title compound, $C_{15}H_{10}I_2O$, is a halogenated chalcone formed from two iodine substituted rings, one *para*-substituted and the other *meta*-substituted, linked through a prop-2-en-1-one spacer. In the molecule, the mean planes of the 3-iodophenyl and the 4-iodophenyl groups are twisted by 46.51 (15)°. The calculated electrostatic potential surfaces show the presence of σ-holes on both substituted iodines. In the crystal, the molecules are linked through type II halogen bonds, forming a sheet structure parallel to the *bc* plane. Between the sheets, weak intermolecular C—H$\cdots\pi$ interactions are observed. Hirshfeld surface analysis showed that the most significant contacts in the structure are C$\cdots$H/H$\cdots$C (31.9%), followed by H$\cdots$H (21.4%), I$\cdots$H/H$\cdots$I (18.4%). I$\cdots$I (14.5%) and O$\cdots$H/H$\cdots$O (8.1%).

1. Chemical context

Chalcones are aromatic ketones which have shown potential as antibacterial, antifungal and anti-inflammatory agents (D'silva *et al.*, 2011). These molecules are essential to the biosynthesis of flavonoids through a conjugate ring-closure to form flavone and have also attracted attention for their potential use in opto- and organic electronics (Shetty *et al.*, 2016, 2017). As a family of molecules, substituted chalcones can be readily synthesized *via* a Claisen–Schmidt condensation reaction between an appropriately functionalized acetophenone and benzaldehyde. Substitutions on each of the benzene rings are currently being investigated in order to interrogate how the electronic properties of the crystal are altered. The iodo-substituted rings present in the title compound allows for the formation of iodine channels in the crystal, a conformation which may afford a change in the crystal's electrical properties.

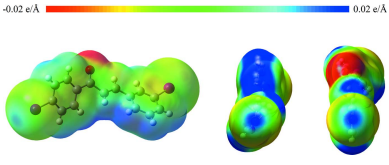

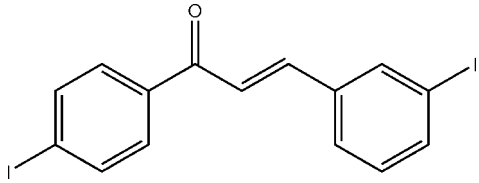

2. Structural commentary

The title compound comprises two aromatic rings, 4-iodophenyl (1-Ring) and 3-iodophenyl (3-Ring), which are

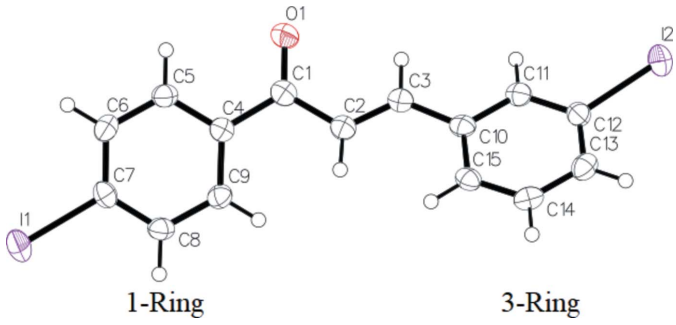

Figure 1
The molecular structure of the title compound, showing the atom labelling and displacement ellipsoids drawn at the 50% probability level.

connected, respectively, to atoms C1 and C3 of the –CO—CH═CH– enone bridge (Fig. 1). The backbone torsion angles are C5—C4—C1—C2 = 151.6 (4)°, C4—C1—C2—C3 = 171.9 (4)°, C1—C2—C3—C10 = 176.4 (4)° and C2—C3—C10—C11 = 170.4 (5)°. The mean planes of the 3-iodophenyl and 4-iodophenyl groups are twisted by 46.51 (15)° relative to each other. The H atoms of the propenone group are *trans*-configured.

3. Supramolecular features

Electrostatic potential surfaces [Fig. 2(*a*)–(*c*)] show the presence of σ-holes on both substituted iodines, I1 and I2, which allow for halogen bonding of a bifurcated type II. Partial packing diagrams are shown in Fig. 3(*a*)–(*c*). Interestingly, these halogen bonds form exclusively between equivalent iodine atoms, either *para–para* or *meta–meta*. The geometries of the halogen bonds are I1···I1^{iv} = 4.0980 (9) Å,

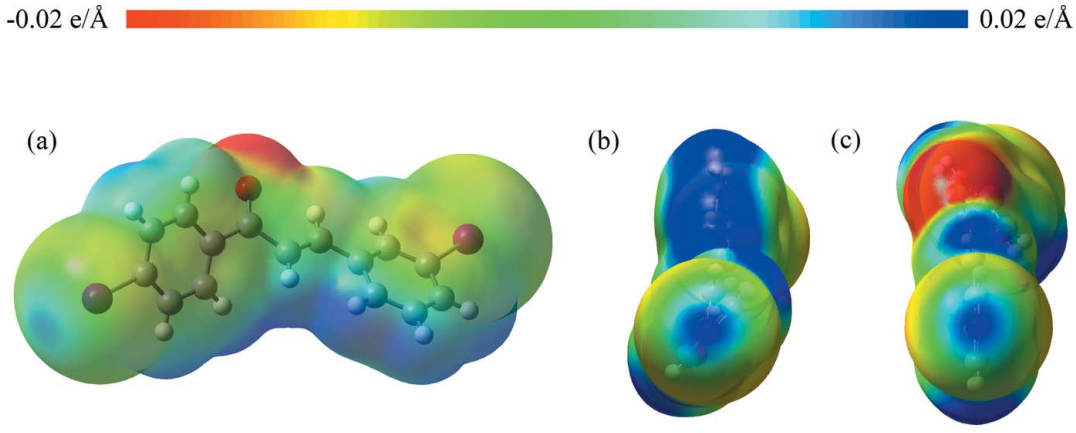

Figure 2
Electrostatic potential mapped onto an electron density isosurface with isovalue 0.02 e Å^{-3}, calculated using B3LYP at the LANL2DZ level. Red and blue regions show negative and positive electric potentials, respectively. (*a*) shows the potential of the substituted chalcone molecule. (*b*) and (*c*) show the σ-holes on 1-Ring and 3-Ring, respectively.

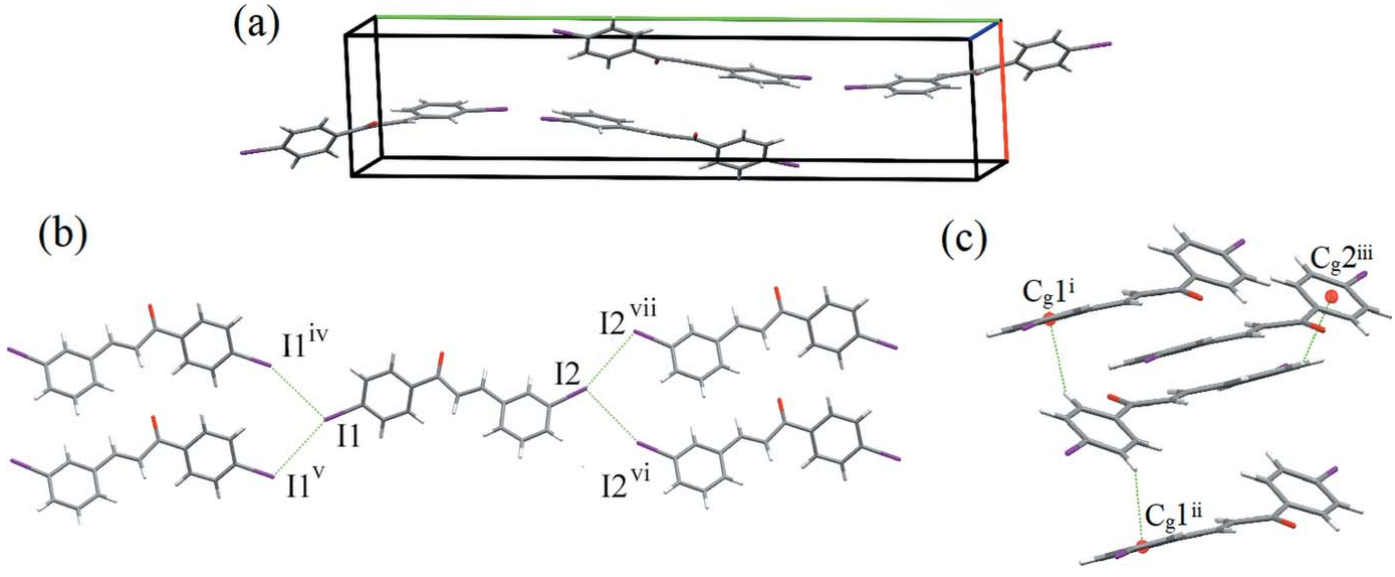

Figure 3
(*a*) A packing diagram of the title compound in the unit cell. Red, green and blue axes indicate *a*, *b* and *c*, respectively. (*b*) *Meta–meta* and *para–para* halogen bonds indicated by dashed lines. (*c*) Three weak C—H···π interactions (dashed lines; C5—H5···*Cg*1^{i}, C8—H8···*Cg*1^{ii} and C14—H14···*Cg*2^{iii}). *Cg*1 and *Cg*2 are the centroids of the C10–C15 and C4–C9 rings, respectively. [Symmetry codes: (i) $1-x, 1-y, 1-z$; (ii) $2-x, 1-y, 2-z$; (iii) $1-x, 1-y, 2-z$; (iv) $x, \frac{1}{2}-y, -\frac{1}{2}+z$; (v) $x, \frac{1}{2}-y, \frac{1}{2}+z$; (vi) $x, \frac{3}{2}-y, \frac{1}{2}+z$; (vii) $x, \frac{3}{2}-y, -\frac{1}{2}+z$..]

Table 1
Hydrogen-bond geometry (Å, °).

*Cg*1 and *Cg*2 are the centroids of the C10–C15 and C4–C9 rings, respectively.

D—H···*A*	*D*—H	H···*A*	*D*···*A*	*D*—H···*A*
C5—H5···*Cg*1^{i}	0.95	2.78	3.406 (5)	124
C8—H8···*Cg*1^{ii}	0.95	2.85	3.491 (5)	126
C14—H14···*Cg*2^{iii}	0.95	2.77	3.440 (5)	129

Symmetry codes: (i) $-x+1, -y+1, -z+1$; (ii) $-x+2, -y+1, -z+2$; (iii) $-x+1, -y+1, -z+2$.

C7—I1···I1^{iv} = 113.85 (13)°, I1···I1^{v} =4.0980 (9) Å and C7—I···I1^{v} = 154.47 (13)° for the *para–para* I···I bonds, and I2···I2^{vi} = 3.9805 (8) Å, C12—I2···I2^{vi} = 108.20 (13)°, I2···I2^{vii} = 3.9805 (8) Å and C12—I2···I2^{vii} = 157.30 (13)° for the *meta–meta* I···I bonds [symmetry codes: (iv) $x, \frac{1}{2}-y, -\frac{1}{2}+z$; (v) $x, \frac{1}{2}-y, \frac{1}{2}+z$; (vi) $x, \frac{3}{2}-y, \frac{1}{2}+z$; (vii) $x, \frac{3}{2}-y, -\frac{1}{2}+z$]. A sheet structure is formed parallel to the *bc* plane. There are also three weak C—H···π interactions (Table 1) between the sheets.

Hirshfeld surfaces, mapped over d_{norm}, shape-index and d_e, and two-dimensional fingerprint plots of the title compound were calculated using *CrystalExplorer17.5* (Turner *et al.*, 2017). Hirshfeld surfaces [Fig. 4(*a*) and (*c*)] highlight the relationship between the contact distance and the van der Waals radii (Venkatesan *et al.*, 2016). The Hirshfeld surface mapped over the shape-index [Fig. 4(*b*)] shows depressions on both 1-Ring and 3-Ring, which is indicative of C—H···π interactions. Two-dimensional fingerprint plots are used to illustrate the intermolecular contacts between molecules within the crystal structure. The fingerprint plots of all significant interactions are shown in Fig. 5(*a*)–(*f*). C···H/H···C contacts [Fig. 5(*b*)]

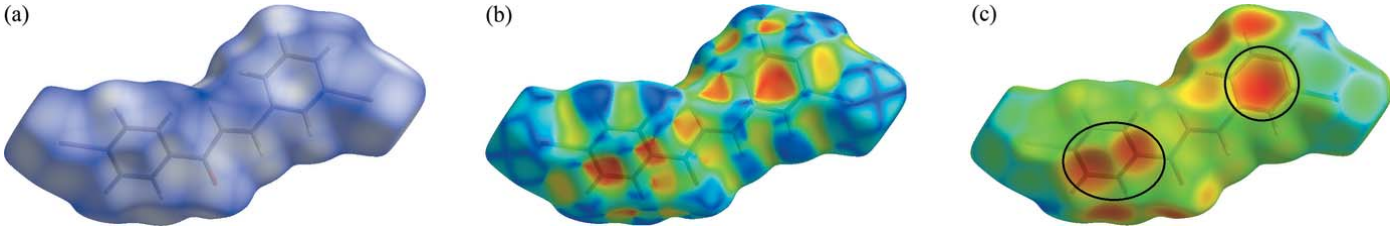

Figure 4
Hirshfeld surfaces of the title compound, mapped with (*a*) d_{norm}, where white regions represent interactions equal to, and blue regions represent interactions shorter than the sum of their van der Waals radii, (*b*) the shape-index, and (*c*) d_e, where the circled areas indicate the C—H···π interactions.

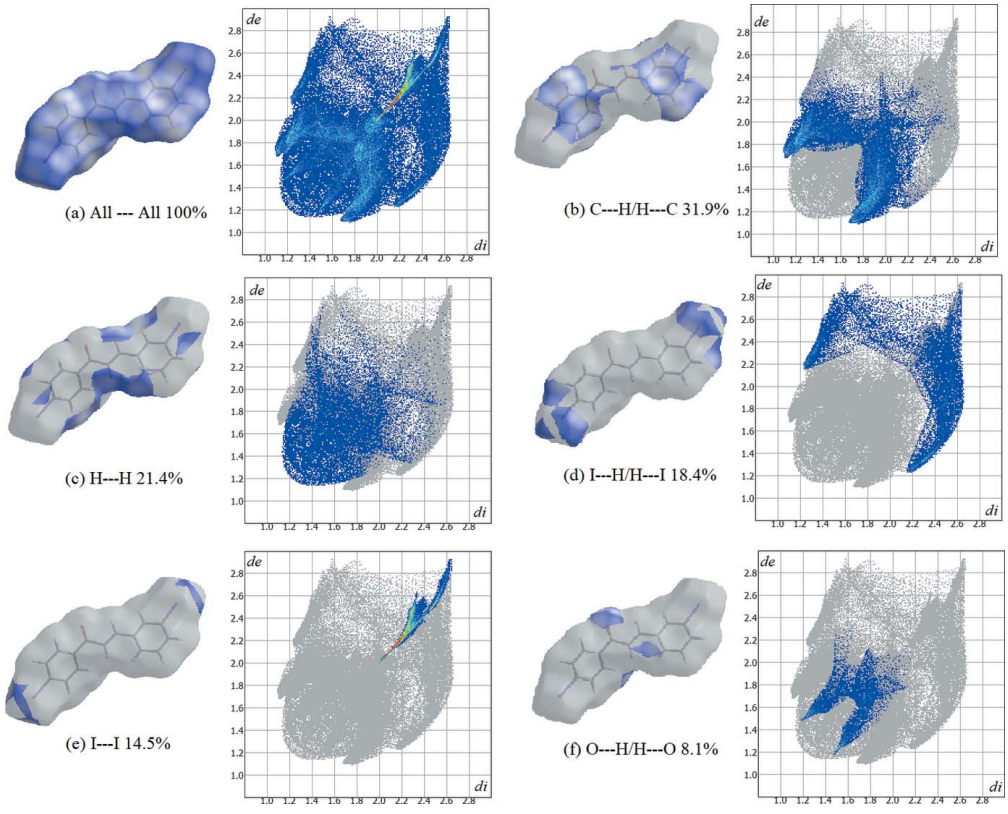

Figure 5
Hirshfeld surfaces and fingerprint plots showing percentage of contacts of (*a*) all interactions, (*b*) C···H/H···C, (*c*) H···H, (*d*) I···H/H···I, (*e*) I···I and (*f*) O···H/H···O. interactions.

Table 2
Experimental details.

Crystal data	
Chemical formula	$C_{15}H_{10}I_2O$
M_r	460.03
Crystal system, space group	Monoclinic, $P2_1/c$
Temperature (K)	200
a, b, c (Å)	7.2650 (7), 32.864 (3), 5.8446 (6)
β (°)	92.277 (2)
V (Å^3)	1394.3 (2)
Z	4
Radiation type	Mo $K\alpha$
μ (mm^{-1})	4.50
Crystal size (mm)	0.57 × 0.29 × 0.08
Data collection	
Diffractometer	Bruker APEXII kappa CCD area detector
Absorption correction	Numerical (*SADABS*; Bruker, 2016)
T_{min}, T_{max}	0.065, 0.189
No. of measured, independent and observed [$I > 2\sigma(I)$] reflections	18346, 3215, 2960
R_{int}	0.021
(sin $\theta/\lambda)_{max}$ (Å^{-1})	0.650
Refinement	
$R[F^2 > 2\sigma(F^2)]$, $wR(F^2)$, S	0.037, 0.073, 1.27
No. of reflections	3215
No. of parameters	164
H-atom treatment	H-atom parameters constrained
$\Delta\rho_{max}$, $\Delta\rho_{min}$ (e Å^{-3})	1.14, −1.31

Computer programs: *SAINT* (Bruker, 2016), *SHELXT* (Sheldrick, 2015*a*), *SHELXL2018* (Sheldrick, 2015*b*) and *OLEX2* (Dolomanov *et al.*, 2009).

make the largest contribution (31.9%) and show a pair of spikes at $d_e + d_i$ = ∼2.8 Å, representative of intermolecular C—H···π interactions. The O···H/H···O plot also contains a pair of spikes at $d_e + d_i$ = ∼2.7 Å [Fig. 5(*f*)]. The negligible contributions from other contacts, not included in Fig. 5, are as follows: C···C (3.1%), C···O/O···C (2.1%) and C···I/I···C (0.5%).

4. Database survey

A survey of the Cambridge Structural Database (CSD; Groom *et al.*, 2016) showed that existing similar structures include (2*E*)-1-(4-bromophenyl)-3-(4-fluorophenyl)prop-2-en-1-one (refcode NURCIN; Dutkiewicz *et al.*, 2010), 1-(4-bromophenyl)-3-(4-chlorophenyl)prop-2-en-1-one (LEPYIP; Yang *et al.*, 2006), 1,3-bis(4-bromophenyl)prop-2-en-1-one (LEHROG; Ng *et al.*, 2006), (*E*)-1-(4-bromophenyl)-3-(4-iodophenyl)prop-2-en-1-one (IWALAV; Zainuri *et al.*, 2017) and 3-(3-bromophenyl)-1-(4-bromophenyl)prop-2-en-1-one (ODEDEH; Teh *et al.*, 2006). Four compounds (NURCIN, LEPYIP, LEHROG and IWALAV) contain only *para*-substituted rings. Within these structures, halogen bonds exist only between bromine and iodine species, and never between equivalent halogens. 3-(3-Bromophenyl)-1-(4-bromophenyl)prop-2-en-1-one contains one *meta*-substituted ring and one *para*-substituted ring: each halogen bond exists between rings with the same substitution, either *para–para* or *meta–meta*, as seen in the title compound.

5. Synthesis and crystallization

4′-Iodoacetophenone (0.773 g, 3.14 mmol), 3-iodobenzaldehyde (0.697 g, 3.00), anhydrous zinc chloride (0.615 g, 4.51 mmol) and absolute ethanol (1.5 ml) were added to a microwave vessel with a stir bar. Using a microwave reactor, the reaction mixture was heated to 468 K for 15 minutes. Upon cooling the reaction, yellowish solids were collected by vacuum filtration and washed with 95% ethanol. The resulting solid was recrystallized from 95% ethanol (0.603 g, 44% yield, yellow crystals, m.p. 442.5–443.7 K). ^{1}H NMR (400 MHz, DMSO-d_6, referenced to TMS): δ (ppm) 8.37 (1H, *s*), 8.0–7.94 (5H, *m*), 7.88 (1H, *d*, J = 8 Hz), 7.81 (1H, *d*, J = 8 Hz), 7.68 (1H, *d*, J = 16 Hz), 7.26 (1H, *t*, J = 8 Hz). ^{13}C NMR (100 MHz, DMSO-d_6, referenced to solvent, 39.52 ppm): δ (ppm) 188.44, 142.75, 139.04, 137.72, 136.95, 136.66, 136.61, 130.89, 130.38, 128.73, 122.81, 102.14, 95.57. Single crystals suitable for X-ray diffraction were obtained by the slow evaporation technique from an acetone solution at room temperature.

6. Refinement

Crystal data, data collection and structure refinement details are summarized in Table 2. H atoms were positioned geometrically (C—H = 0.95 Å) and refined using a riding model with U_{iso}(H) = 1.2U_{eq}(C).

Acknowledgements

GU co-authors thank E. Mermann-Jozwiak, J. Hazen, S. Economu, M. Fellin, B. Hendricks, R. Meehan, & G. Warren for their assistance, as well as the Howard Hughes Medical Institute through its Undergraduate Science Education Program for supporting equipment acquisition.

Funding information

UoB co-authors acknowledge the Engineering and Physical Sciences Research Council UK (grant EP/G036780/1) and the Centre for Doctoral Training in Condensed Matter Physics for project funding. SRH and JP acknowledge MagnaPharm, a collaborative research project funded by the European Union's Horizon 2020 Research and Innovation programme (grant No. 736899).

References

Bruker (2016). *SAINT* and *SADABS*. Bruker Analytical X-ray Instruments Inc., Madison, WI, USA.

Dolomanov, O. V., Bourhis, L. J., Gildea, R. J., Howard, J. A. K. & Puschmann, H. (2009). *J. Appl. Cryst.* **42**, 339–341.

D'silva, E. D., Podagatlapalli, G. K., Rao, S. V., Rao, D. N. & Dharmaprakash, S. M. (2011). *Cryst. Growth Des.* **11**, 5326–5369.

Dutkiewicz, G., Veena, K., Narayana, B., Yathirajan, H. S. & Kubicki, M. (2010). *Acta Cryst.* E**66**, o1243–o1244.

Groom, C. R., Bruno, I. J., Lightfoot, M. P. & Ward, S. C. (2016). *Acta Cryst.* B**72**, 171–179.

Ng, S.-L., Shettigar, V., Razak, I. A., Fun, H.-K., Patil, P. S. & Dharmaprakash, S. M. (2006). *Acta Cryst.* E**62**, o1421–o1423.

Sheldrick, G. M. (2015*a*). *Acta Cryst.* A**71**, 3–8.

Sheldrick, G. M. (2015*b*). *Acta Cryst.* C**71**, 3–8.

Shetty, T. C. S., Chidan Kumar, C. S., Gagan Patel, K. N., Chia, T. S., Dharmaprakash, S. M., Ramasami, P., Umar, Y., Chandraju, S. & Quah, C. K. (2017). *J. Mol. Struct*. **1143**, 306–317.
Shetty, T. C. S., Raghavendra, S., Chidan Kumar, C. S. & Dharmaprakash, S. M. (2016). *Appl. Phys. B*, **122**, 205.
Teh, J. B.-J., Patil, P. S., Fun, H.-K., Razak, I. A. & Dharmaprakash, S. M. (2006). *Acta Cryst.* E**62**, o2399–o2400.
Turner, M. J., McKinnon, J. J., Wolff, S. K., Grimwood, D. J., Spackman, P. R., Jayatilaka, D. & Spackman, M. A. (2017). *CrystalExplorer.* Version 17. University of Western Australia.
Venkatesan, P., Thamotharan, S., Ilangovan, A., Liang, H. & Sundius, T. (2016). *Spectrochim. Acta Part A*, **153**, 625–636.
Yang, W., Wang, L. & Zhang, D. (2006). *J. Chem. Crystallogr.* **36**, 195–198.
Zainuri, D. A., Arshad, S., Khalib, N. C., Razak, I. A., Pillai, R. R., Sulaiman, S. F., Hashim, N. S., Ooi, K. L., Armaković, S., Armaković, S. J., Panicker, C. Y. & Van Alsenoy, C. (2017). *J. Mol. Struct.* **1128**, 520–533.

supporting information

Acta Cryst. (2020). E**76**, 72-76 [https://doi.org/10.1107/S2056989019016402]

Crystal structure and Hirshfeld surface analysis of (*E*)-3-(3-iodophenyl)-1-(4-iodophenyl)prop-2-en-1-one

Kieran J. Spruce, Charlie L. Hall, Jason Potticary, Natalie E. Pridmore, Matthew E. Cremeens, Gemma D. D'ambruoso, Masaomi Matsumoto, Gabrielle I. Warren, Stephen D. Warren and Simon R. Hall

Computing details

Data collection: *SAINT* (Bruker, 2016); cell refinement: *SAINT* (Bruker, 2016); data reduction: *SAINT* (Bruker, 2016); program(s) used to solve structure: SHELXT (Sheldrick, 2015*a*); program(s) used to refine structure: *SHELXL2018* (Sheldrick, 2015*b*); molecular graphics: *OLEX2* (Dolomanov *et al.*, 2009); software used to prepare material for publication: *OLEX2* (Dolomanov *et al.*, 2009).

(*E*)-3-(3-Iodophenyl)-1-(4-iodophenyl)prop-2-en-1-one

Crystal data

$C_{15}H_{10}I_2O$
$M_r = 460.03$
Monoclinic, $P2_1/c$
$a = 7.2650$ (7) Å
$b = 32.864$ (3) Å
$c = 5.8446$ (6) Å
$\beta = 92.277$ (2)°
$V = 1394.3$ (2) Å^3
$Z = 4$
$F(000) = 856$
$D_x = 2.191$ Mg m^{-3}
Mo $K\alpha$ radiation, $\lambda = 0.71073$ Å
Cell parameters from 8513 reflections
$\theta = 2.5$–27.5°
$\mu = 4.50$ mm^{-1}
$T = 200$ K
Plate, clear colourless
0.57 × 0.29 × 0.08 mm

Data collection

Bruker APEXII kappa CCD area detector diffractometer
Radiation source: fine-focus sealed tube
Graphite monochromator
φ and ω scans
Absorption correction: numerical (SADABS; Bruker, 2016)
$T_{min} = 0.065$, $T_{max} = 0.189$
18346 measured reflections
3215 independent reflections
2960 reflections with $I > 2\sigma(I)$
$R_{int} = 0.021$
$\theta_{max} = 27.5°$, $\theta_{min} = 2.5°$
$h = -9\rightarrow9$
$k = -42\rightarrow37$
$l = -7\rightarrow7$

Refinement

Refinement on F^2
Least-squares matrix: full
$R[F^2 > 2\sigma(F^2)] = 0.037$
$wR(F^2) = 0.073$
$S = 1.27$
3215 reflections
164 parameters
0 restraints
Primary atom site location: iterative
Hydrogen site location: inferred from neighbouring sites
H-atom parameters constrained

$w = 1/[\sigma^2(F_o^2) + (0.0034P)^2 + 6.4729P]$
where $P = (F_o^2 + 2F_c^2)/3$
$(\Delta/\sigma)_{max} = 0.001$
$\Delta\rho_{max} = 1.14$ e Å^{-3}
$\Delta\rho_{min} = -1.30$ e Å^{-3}

Extinction correction: SHELXL2018 (Sheldrick, 2015*b*), $Fc^* = kFc[1+0.001xFc^2\lambda^3/\sin(2\theta)]^{-1/4}$
Extinction coefficient: 0.00062 (7)

Special details

Geometry. All esds (except the esd in the dihedral angle between two l.s. planes) are estimated using the full covariance matrix. The cell esds are taken into account individually in the estimation of esds in distances, angles and torsion angles; correlations between esds in cell parameters are only used when they are defined by crystal symmetry. An approximate (isotropic) treatment of cell esds is used for estimating esds involving l.s. planes.

Fractional atomic coordinates and isotropic or equivalent isotropic displacement parameters (Å²)

	x	*y*	*z*	U_{iso}*/U_{eq}
C4	0.8336 (6)	0.43230 (13)	0.5707 (7)	0.0250 (9)
C9	0.9114 (6)	0.42521 (14)	0.7892 (8)	0.0278 (9)
H9	0.939830	0.447424	0.888449	0.033*
C8	0.9474 (6)	0.38548 (14)	0.8617 (8)	0.0289 (9)
H8	1.003866	0.380553	1.008533	0.035*
C7	0.9004 (6)	0.35322 (14)	0.7183 (8)	0.0292 (9)
C6	0.8265 (6)	0.35974 (14)	0.4992 (8)	0.0298 (10)
H6	0.797488	0.337429	0.400879	0.036*
C5	0.7955 (6)	0.39954 (14)	0.4252 (8)	0.0285 (9)
H5	0.747935	0.404397	0.273958	0.034*
C1	0.7892 (6)	0.47421 (14)	0.4874 (8)	0.0284 (9)
C2	0.7447 (6)	0.50560 (14)	0.6605 (8)	0.0294 (9)
H2	0.729579	0.497837	0.815221	0.035*
C3	0.7258 (6)	0.54438 (13)	0.5999 (8)	0.0268 (9)
H3	0.749373	0.550781	0.445302	0.032*
C10	0.6729 (6)	0.57825 (13)	0.7450 (7)	0.0251 (9)
C11	0.6878 (6)	0.61791 (13)	0.6589 (8)	0.0273 (9)
H11	0.740192	0.622248	0.514565	0.033*
C12	0.6264 (6)	0.65086 (13)	0.7836 (8)	0.0289 (9)
C13	0.5540 (6)	0.64548 (15)	0.9989 (8)	0.0322 (10)
H13	0.513741	0.668101	1.084900	0.039*
C14	0.5424 (6)	0.60607 (15)	1.0845 (8)	0.0311 (10)
H14	0.493446	0.601952	1.230991	0.037*
C15	0.6003 (6)	0.57271 (14)	0.9618 (8)	0.0280 (9)
H15	0.590951	0.546131	1.024224	0.034*
I1	0.92866 (6)	0.29371 (2)	0.84509 (7)	0.04484 (12)
I2	0.63173 (6)	0.70888 (2)	0.63477 (6)	0.04434 (12)
O1	0.7830 (5)	0.48192 (10)	0.2821 (6)	0.0376 (8)

Atomic displacement parameters (Å²)

	U^{11}	U^{22}	U^{33}	U^{12}	U^{13}	U^{23}
C4	0.022 (2)	0.027 (2)	0.026 (2)	0.0011 (17)	0.0023 (16)	0.0009 (17)
C9	0.027 (2)	0.028 (2)	0.028 (2)	−0.0020 (18)	−0.0031 (18)	−0.0029 (17)

C8	0.028 (2)	0.034 (2)	0.024 (2)	0.0032 (19)	−0.0031 (17)	0.0017 (18)
C7	0.027 (2)	0.026 (2)	0.034 (2)	0.0048 (18)	0.0022 (18)	0.0026 (18)
C6	0.029 (2)	0.029 (2)	0.031 (2)	0.0003 (18)	−0.0001 (18)	−0.0077 (18)
C5	0.028 (2)	0.033 (2)	0.024 (2)	0.0036 (18)	−0.0010 (17)	−0.0009 (17)
C1	0.023 (2)	0.031 (2)	0.031 (2)	0.0005 (17)	0.0008 (18)	0.0024 (18)
C2	0.033 (2)	0.028 (2)	0.027 (2)	−0.0004 (18)	0.0022 (18)	0.0019 (17)
C3	0.026 (2)	0.029 (2)	0.026 (2)	−0.0005 (18)	0.0003 (17)	0.0016 (17)
C10	0.021 (2)	0.030 (2)	0.025 (2)	−0.0016 (17)	−0.0045 (16)	0.0015 (17)
C11	0.027 (2)	0.029 (2)	0.026 (2)	−0.0048 (18)	−0.0012 (17)	0.0022 (17)
C12	0.031 (2)	0.024 (2)	0.031 (2)	−0.0037 (18)	−0.0077 (18)	0.0016 (17)
C13	0.028 (2)	0.035 (2)	0.033 (2)	0.0014 (19)	−0.0018 (19)	−0.0073 (19)
C14	0.028 (2)	0.041 (3)	0.024 (2)	−0.002 (2)	−0.0003 (18)	−0.0015 (19)
C15	0.025 (2)	0.030 (2)	0.028 (2)	0.0001 (18)	−0.0048 (17)	0.0043 (18)
I1	0.0555 (2)	0.02652 (17)	0.0520 (2)	0.00766 (15)	−0.00426 (16)	0.00411 (14)
I2	0.0618 (3)	0.02421 (16)	0.0466 (2)	−0.00405 (15)	−0.00256 (16)	0.00229 (14)
O1	0.051 (2)	0.0340 (18)	0.0278 (17)	0.0045 (16)	0.0029 (15)	0.0051 (14)

Geometric parameters (Å, º)

C4—C9	1.395 (6)	C2—C3	1.328 (6)
C4—C5	1.393 (6)	C3—H3	0.9500
C4—C1	1.492 (6)	C3—C10	1.460 (6)
C9—H9	0.9500	C10—C11	1.403 (6)
C9—C8	1.394 (6)	C10—C15	1.403 (6)
C8—H8	0.9500	C11—H11	0.9500
C8—C7	1.386 (6)	C11—C12	1.388 (6)
C7—C6	1.386 (6)	C12—C13	1.394 (7)
C7—I1	2.099 (4)	C12—I2	2.097 (4)
C6—H6	0.9500	C13—H13	0.9500
C6—C5	1.393 (6)	C13—C14	1.392 (7)
C5—H5	0.9500	C14—H14	0.9500
C1—C2	1.490 (6)	C14—C15	1.385 (7)
C1—O1	1.225 (5)	C15—H15	0.9500
C2—H2	0.9500		

C9—C4—C1	121.8 (4)	C3—C2—H2	119.8
C5—C4—C9	119.5 (4)	C2—C3—H3	116.4
C5—C4—C1	118.6 (4)	C2—C3—C10	127.1 (4)
C4—C9—H9	120.0	C10—C3—H3	116.4
C8—C9—C4	119.9 (4)	C11—C10—C3	118.3 (4)
C8—C9—H9	120.0	C11—C10—C15	118.8 (4)
C9—C8—H8	120.2	C15—C10—C3	122.8 (4)
C7—C8—C9	119.6 (4)	C10—C11—H11	119.8
C7—C8—H8	120.2	C12—C11—C10	120.4 (4)
C8—C7—I1	118.8 (3)	C12—C11—H11	119.8
C6—C7—C8	121.2 (4)	C11—C12—C13	121.0 (4)
C6—C7—I1	120.0 (3)	C11—C12—I2	118.7 (3)
C7—C6—H6	120.5	C13—C12—I2	120.2 (3)

C7—C6—C5	118.9 (4)	C12—C13—H13	120.9
C5—C6—H6	120.5	C14—C13—C12	118.2 (4)
C4—C5—C6	120.7 (4)	C14—C13—H13	120.9
C4—C5—H5	119.6	C13—C14—H14	119.1
C6—C5—H5	119.6	C15—C14—C13	121.8 (4)
C2—C1—C4	117.9 (4)	C15—C14—H14	119.1
O1—C1—C4	120.6 (4)	C10—C15—H15	120.1
O1—C1—C2	121.4 (4)	C14—C15—C10	119.8 (4)
C1—C2—H2	119.8	C14—C15—H15	120.1
C3—C2—C1	120.4 (4)		

C4—C9—C8—C7	−1.9 (7)	C2—C3—C10—C11	170.4 (5)
C4—C1—C2—C3	171.9 (4)	C2—C3—C10—C15	−12.5 (7)
C9—C4—C5—C6	2.9 (7)	C3—C10—C11—C12	175.2 (4)
C9—C4—C1—C2	−28.3 (6)	C3—C10—C15—C14	−176.0 (4)
C9—C4—C1—O1	154.5 (5)	C10—C11—C12—C13	1.9 (7)
C9—C8—C7—C6	3.3 (7)	C10—C11—C12—I2	−175.0 (3)
C9—C8—C7—I1	−173.2 (3)	C11—C10—C15—C14	1.0 (6)
C8—C7—C6—C5	−1.5 (7)	C11—C12—C13—C14	−0.9 (7)
C7—C6—C5—C4	−1.6 (7)	C12—C13—C14—C15	0.0 (7)
C5—C4—C9—C8	−1.1 (7)	C13—C14—C15—C10	0.0 (7)
C5—C4—C1—C2	151.6 (4)	C15—C10—C11—C12	−1.9 (6)
C5—C4—C1—O1	−25.6 (7)	I1—C7—C6—C5	175.0 (3)
C1—C4—C9—C8	178.8 (4)	I2—C12—C13—C14	175.9 (3)
C1—C4—C5—C6	−177.0 (4)	O1—C1—C2—C3	−10.9 (7)
C1—C2—C3—C10	176.4 (4)		

Hydrogen-bond geometry (Å, º)

*Cg*1 and *Cg*2 are the centroids of the C10–C15 and C4–C9 rings, respectively.

D—H···*A*	*D*—H	H···*A*	*D*···*A*	*D*—H···*A*
C5—H5···*Cg*1^{i}	0.95	2.78	3.406 (5)	124
C8—H8···*Cg*1^{ii}	0.95	2.85	3.491 (5)	126
C14—H14···*Cg*2^{iii}	0.95	2.77	3.440 (5)	129

Symmetry codes: (i) −*x*+1, −*y*+1, −*z*+1; (ii) −*x*+2, −*y*+1, −*z*+2; (iii) −*x*+1, −*y*+1, −*z*+2.